Theory of Dielectric Elastomers Capable of Giant Deformation of Actuation

Xuanhe Zhao and Zhigang Suo*

School of Engineering and Applied Sciences, Harvard University, Cambridge, Massachusetts 02138, USA

(Received 21 January 2010; published 30 April 2010)

The deformation of a dielectric induced by voltage is limited by electrical breakdown if the dielectric is stiff, and by electromechanical instability if the dielectric is compliant. The interplay of the two modes of instability is analyzed for a dielectric elastomer, which is compliant at a small stretch, but stiffens steeply. The theory is illustrated with recent experiments of interpenetrating networks, and with a model of swollen elastomers. The theory predicts that, for an elastomer with a stress-stretch curve of a desirable form, the voltage can induce giant deformation.

DOI: 10.1103/PhysRevLett.104.178302 PACS numbers: 82.35.Lr, 61.41.+e, 77.84.Jd

Subject to a voltage, a membrane of a dielectric elastomer reduces thickness and expands area. This phenomenon is being studied intensely in the emerging technology of elastomeric transducers. Applications include artificial muscles, tunable optics, generators for harvesting energy, and tactile sensors for Braille displays [1–4]. The elastomeric transducers have remarkable attributes such as high specific energy, fast response, and negligible noise. This Letter focuses on the most conspicuous attribute: large deformation of actuation induced by voltage.

While all dielectrics deform under voltage, the attainable deformation of actuation varies markedly. Piezoelectric ceramics attain strains of actuation typically less than 1% [5]. Glassy and semicrystalline polymers can attain less than 10% [6]. The initial reported values for elastomers were a few percent [7]. By using soft electrodes, strains of actuation about 30% were observed in some elastomers [8]. In the past decade, strains over 100% have been achieved in several ways, by prestretching an elastomer [9], by using an elastomer of interpenetrating networks [10], by swelling an elastomer with a solvent [11], and by spraying charge on an electrode-free elastomer [12].

These experimental advances have prompted a theoretical question: What is the fundamental limit of deformation of actuation? A theory may interpret the diverse and intriguing experimental observations mentioned above, and guide the search for dielectrics of even larger deformation of actuation. This Letter presents a theory to show that dielectric elastomers are capable of giant deformation of actuation, beyond 100%.

For a stiff dielectric such as a ceramic or a glassy polymer, deformation of actuation is limited by electrical breakdown, when the voltage mobilizes charged species in the dielectric to produce a path of electrical conduction [13]. For a compliant dielectric such as an elastomer, the deformation of actuation is often limited by electromechanical instability, when the voltage causes the dielectric to thin down excessively [14,15]. After electromechanical instability, the electric field increases as the membrane thins until the dielectric fails by electrical breakdown. In addition to these two types of behavior, which we call type I and type II, the theory will suggest a type III behavior: the dielectric eliminates or survives electromechanical instability, reaches a stable state without electrical breakdown, and attains large deformation of actuation.

Figure 1(a) sketches a dielectric membrane pulled by biaxial stresses σ. The length of the membrane in any direction in the plane is stretched by a ratio λ. As will become clear, a type III dielectric should have a stress-stretch curve $\sigma(\lambda)$ of the following desirable features: (a) The dielectric is compliant at small stretches, and (b) the dielectric stiffens steeply at modest stretches. That is, the limiting stretch λ_{lim} should not be excessive. Also sketched are several designs of materials that exhibit the stress-stretch curve of the desirable form. Many bio-

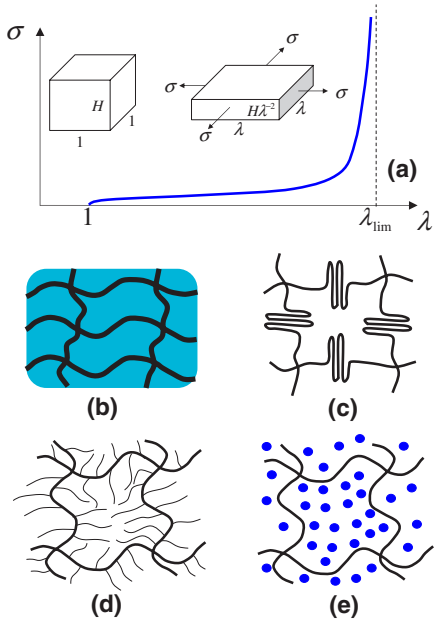

FIG. 1 (color online). (a) Stress-stretch curve of a membrane under biaxial stresses. (b) Fibers embedded in a compliant matrix. (c) A network of polymers with folded domains. (d) A network of polymers with side chains. (e) A network of polymers swollen with a solvent.

logical tissues, such as skins and vascular walls, deform readily, but avert excessive deformation [16]. Figure 1(b) sketches a design of such a tissue, consisting of stiffer fibers in a compliant matrix. At small stretches, the fibers are loose, and the tissue is compliant. At large stretches, the fibers are taut, and the tissue stiffens steeply. As another example, Fig. 1(c) sketches a network of polymers with folded domains [17]. The domains unfold when the network is pulled, giving rise to substantial deformation. After all the domains unfold, the network stiffens steeply.

Consider a synthetic elastomer, i.e., a network of polymer chains. When the individual chains are short, the initial modulus of the elastomer is large and the limiting stretch λ_{lim} is small. When the individual chains are long, the initial modulus of the elastomer is small and the limiting stretch λ_{lim} is large. Consequently, it is difficult to achieve the stress-stretch curve of the desirable form by adjusting the density of cross-links alone. The stress-stretch curve, however, can be shaped into the desirable form in several ways. For example, the widely used dielectric elastomer, VHB (a tape from 3M Company), is a network of polymers with side chains [Fig. 1(d)] [18]. The side chains fill the space around the networked chains. The motion of the networked chains is lubricated, lowering the glass transition temperature. Also the density of the networked chains is reduced, lowering the stiffness of the elastomer when the stretch is small. While the side chains do not change the contour length of the networked chains, the side chains pull the networked chains towards their full contour length even when the elastomer is not loaded. Once loaded, the elastomer may stiffen sharply, averting electromechanical instability. Similar behavior is expected for a network swollen with a solvent [Fig. 1(e)] [19]. The stress-stretch curve can also be shaped into the desirable form by prestretch [9], or by using interpenetrating networks [10,20].

Figure 2(a) illustrates the working principle of dielectric elastomer transducers. When a membrane of an elastomer, thickness H in the undeformed state, is subject to a voltage Φ, the membrane is stretched by λ in both directions in the plane, the thickness of the membrane reduces to $H\lambda^{-2}$, and the electric field in the membrane is $E = \lambda^2\Phi/H$. The membrane is taken to be incompressible. The actuation can be described by the Maxwell stress, $\sigma = \varepsilon E^2$, where ε is the permittivity of the elastomer [8]. The use of the Maxwell stress assumes that the dielectric behavior of the elastomer is liquidlike, unaffected by deformation. This material model, known as the ideal dielectric elastomer [21,22], has been confirmed experimentally [23], and used almost exclusively in the literature on dielectric elastomers (e.g., Refs. [1–4,8–15]). A recent experiment, however, showed that the permittivity of a dielectric elastomer varied about a factor of 2 when the area of the membrane was stretched by a factor of 25 [24]. This variation has been included in a theoretical analysis [22]. The resulting equations are more complicated, but do not change the physical picture here. In this Letter, to focus on essential ideas, we will adopt the model of ideal dielectric elastomer.

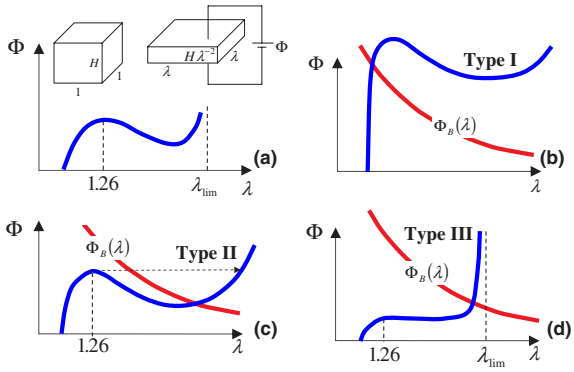

FIG. 2 (color online). (a) A membrane of a dielectric elastomer subject to a voltage reduces thickness and expands area. The voltage-stretch curve is typically not monotonic. (b)–(d) Three types of dielectrics are distinguished, depending on where the two curves $\Phi(\lambda)$ and $\Phi_B(\lambda)$ intersect.

A combination of the above considerations relates the voltage to the stretch:

$$\Phi = H\lambda^{-2}\sqrt{\sigma(\lambda)/\varepsilon}. \tag{1}$$

This relation is sketched in Fig. 2(a). Even though the stress-stretch curve $\sigma(\lambda)$ is monotonic, the voltage-stretch curve $\Phi(\lambda)$ is usually not [21]. At a small stretch ($\lambda \sim 1$), the rising $\sigma(\lambda)$ dominates, and the voltage increases with the stretch. At an intermediate stretch, the factor λ^{-2} due to thinning of the membrane becomes important, and the voltage falls as the stretch increases. As the elastomer approaches the limiting stretch λ_{lim}, the steep rise of $\sigma(\lambda)$ prevails, and the voltage rises again. The shape of the voltage-stretch curve $\Phi(\lambda)$ indicates a snap-through electromechanical instability [21]. The instability can cause some regions of the elastomer to thin down more than others [25,26].

Before a voltage is applied, an elastomer may be prestretched to λ by a mechanical force, and then fixed by rigid electrodes. Subsequently, when the voltage is applied, the elastomer will not deform further. The measured voltage at failure is taken to be the electrical breakdown voltage. Experiments indicate that the breakdown voltage is a monotonically decreasing function of the prestretch $\Phi_B(\lambda)$ [23,27]. This trend may be interpreted as follows. In terms of the electrical breakdown field E_B, the breakdown voltage is $\Phi_B = E_B H\lambda^{-2}$. For an ideal dielectric elastomer, the dielectric behavior is liquidlike, and E_B is independent of deformation, so that the breakdown voltage scales with the stretch as $\Phi_B \propto \lambda^{-2}$. The experimental data show that Φ_B for dielectric elastomers decreases less steeply than λ^{-2}, indicating that E_B increases with λ. This dependence of the breakdown field on the prestretch is not understood, but will not affect the physical content of our theory. For simplicity, we will assume that E_B is independent of deformation in numerical calculations.

According to where the curves $\Phi(\lambda)$ and $\Phi_B(\lambda)$ intersect, we distinguish three types of dielectrics. A type I

dielectric suffers electrical breakdown prior to electromechanical instability, and is capable of small deformation of actuation; Fig. 2(b). A type II dielectric reaches the peak of the $\Phi(\lambda)$ curve, and thins down excessively, leading to electrical breakdown; Fig. 2(c). The dielectric is recorded to fail at the peak of $\Phi(\lambda)$, which can be much below the breakdown voltage Φ_B. The deformation of actuation is limited by the stretch at which the voltage reaches the peak. A type III dielectric eliminates or survives electromechanical instability, reaches a stable state before the electrical breakdown, and attains a large deformation of actuation; Fig. 2(d). For a dielectric that survives the snap-through electromechanical instability, there will be a gap in the achievable stretches of actuation: the voltage can control stretches of small and large values, but not the intermediate ones.

This theory accounts for the diverse experimental observations mentioned at the beginning of the Letter. As an illustration, Fig. 3(a) plots the stress-stretch curves for VHB and for VHB-Trimethylolpropane trimethacrylate (TMPPMA) interpenetration networks, using available experimental data [28]. Substituting these stress-stretch curves into Eq. (1), we plot the voltage-stretch curves $\Phi(\lambda)$; Fig. 3(b). Also included in Fig. 3(b) is the curve $\Phi_B(\lambda)$, plotted using the representative experimental values $H \approx 1$ mm, $E_B \approx 4 \times 10^8$ V/m, and $\varepsilon \approx 4 \times 10^{-11}$ F/m [1]. The VHB is compliant and stiffens slowly, but the VHB-TMPPMA stiffens steeply. The voltage-stretch curve indicates that the VHB is a type II dielectric, and attains a stretch of actuation about $\lambda \approx 1.26$. By contrast, the voltage-stretch curve indicates that the VHB-TMPPMA is a type III dielectric, and attains a stretch of actuation about $\lambda \approx 2$. These theoretical results agree with experimental observations [28].

To illustrate the potential of the theory, consider a network of polymers swollen with a solvent [Fig. 1(e)]. The existing experimental papers on swollen dielectric elastomers did not report stress-stretch curves in the stiffening region [11,19]. Instead, here we adopt a well-known model that represents the network in which every chain deforms by the same amount [29], and represents each individual chain by freely jointed links [30].

Let λ_1, λ_2, and λ_3 be the stretches of the elastomer relative to the unstressed swollen elastomer. We assume that the volumes of the networked polymers and the solvent molecules do not vary during actuation, so that the swollen elastomer is incompressible, $\lambda_1\lambda_2\lambda_3 = 1$. Let α^3 be the volume of the swollen elastomer divided by the volume of the dry network, so that the stretches of the elastomer relative to the dry network are $\alpha\lambda_1$, $\alpha\lambda_2$, and $\alpha\lambda_3$. Let Λ be the stretch of each chain [29]. In the presence of the solvent,

$$\Lambda = \alpha(\lambda_1^2 + \lambda_2^2 + \lambda_3^2)^{1/2}/\sqrt{3}. \tag{2}$$

For a chain of n links, the stretch Λ relates to the normalized force ζ as [30]

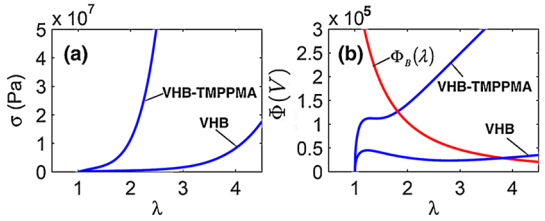

FIG. 3 (color online). (a) Stress-stretch curves for VHB and for VHB-TMPPMA interpenetrating networks plotted using experimental data [28]. (b) Voltage-stretch curves for the two materials plotted according to Eq. (1).

$$\Lambda = \sqrt{n}(\zeta/\tanh\zeta - 1)/\zeta. \tag{3}$$

The free energy per unit volume of the swollen elastomer is

$$W = \frac{kT}{\upsilon\alpha^3}\left(\frac{\zeta}{\tanh\zeta} + \log\frac{\zeta}{\sinh\zeta}\right), \tag{4}$$

where kT is the temperature in the unit of energy, and υ the volume per link. As mentioned above, we have assumed that the amount of the solvent in the elastomer does not change during actuation. The free energy of mixing the network and the solvent depends on the amount of the solvent, but is invariant when the elastomer changes shape. Consequently, the free energy of mixing is not included in (4). To focus on main ideas, we have not included delicate effects of coupling between swelling and chain stretching.

Equations (2)–(4) define the function $W(\lambda_1, \lambda_2)$ using two intermediate variables, ζ and Λ. For an elastomer under triaxial stresses σ_1, σ_2, and σ_3, the equations of state are $\sigma_1 - \sigma_3 = \lambda_1\partial W(\lambda_1, \lambda_2)/\partial\lambda_1$ and $\sigma_2 - \sigma_3 = \lambda_2\partial W(\lambda_1, \lambda_2)/\partial\lambda_2$ [30]. Under biaxial stresses, $\sigma_1 = \sigma_2 = \sigma$ and $\sigma_3 = 0$, we obtain that $\lambda_1 = \lambda_2 = \lambda$ and $\lambda_3 = \lambda^{-2}$, as well as the stress-stretch curve

$$\sigma(\lambda) = \frac{kT\zeta(\lambda^2 - \lambda^{-4})}{3\alpha\upsilon\sqrt{n}\Lambda}. \tag{5}$$

The solvent modifies the stress-stretch curve of the elastomer into the desirable form by reducing both the limiting stretch $\lambda_{\lim}$ and the initial modulus μ. In one limit, as $\lambda \to \lambda_{\lim}$, the chain approaches the full contour length, so that $\Lambda \to \sqrt{n}$. Under the biaxial stress, the limiting stretch is determined by $\alpha(2\lambda^2 + \lambda^{-4})^{1/2}/\sqrt{3} \to \sqrt{n}$, or $\lambda_{\lim} \approx \alpha^{-1}\sqrt{3n/2}$. In the other limit, the chain coils much below the full contour length, so that $\Lambda \ll \sqrt{n}$. The model becomes $W = (kT/6\alpha^3\upsilon)\zeta^2$ and $\Lambda = (\sqrt{n}/3)\zeta$, which recovers the neo-Hookean model, with the initial modulus $\mu = kT/(\upsilon n\alpha)$.

The curve $\Phi(\lambda)$ can be obtained by combining (1) and (5). Figure 4(a) plots $\Phi(\lambda)$ for several values of n for a dry network ($\alpha = 1$). Also plotted is the condition for electrical breakdown $\Phi_B = E_B H\lambda^{-2}$. We have used representative values $E_B = 2 \times 10^8$ V/m, $T = 300$ K, $\upsilon = 10^{-27}$ m^3, $\varepsilon = 4 \times 10^{-11}$ F/m, and $H = 1$ mm [23,27]. To account for the uncertainty of the available experimental data, we have used a conservative value for

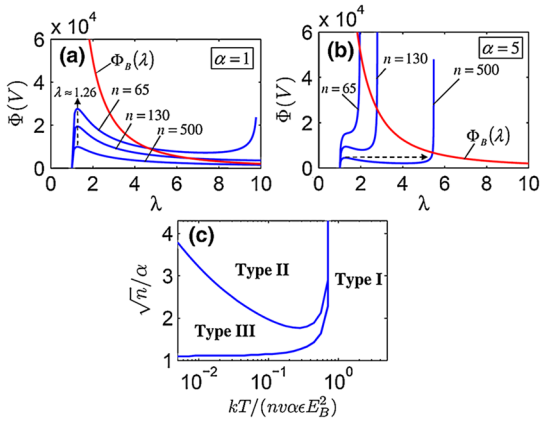

FIG. 4 (color online). (a) A dry elastomer fails by electromechanical instability, and attains deformation of actuation about 1.26. (b) An elastomer swollen with a solvent eliminates or survives electromechanical instability, and attains a large deformation of actuation. (c) Regimes of the three types of dielectrics plotted on the plane spanned by two dimensionless parameters.

the breakdown field E_B. For various values of n, type II behavior occurs, where the elastomer fails by electromechanical instability, and the stretch of actuation is $\lambda \approx 1.26$. Figure 4(b) plots the voltage-stretch curves $\Phi(\lambda)$ for several values of n for a swollen elastomer ($\alpha = 5$). Here type III behavior occurs, where the elastomer eliminates or survives the electromechanical instability. The stretch of actuation reaches $\lambda \approx 2$ for $n = 65$, and reaches $\lambda \approx 5.5$ when $n = 500$. Moreover, for the elastomer that survives the instability (e.g., $n = 500$), there is a gap in the achievable stretches of actuation.

The model of swollen elastomers is characterized by two dimensionless numbers: $\sqrt{n}/\alpha$ scales with the limiting stretch, and $kT/(\upsilon n \alpha \varepsilon E_B^2)$ is the ratio of the initial modulus over the Maxwell stress at electrical breakdown. Figure 4(c) uses the two numbers as the axes for a plane, in which the regimes of the three types of dielectrics are marked. Type I dielectrics have large initial moduli. Type II dielectrics have small initial moduli and excessive limiting stretches. Type III dielectrics have small initial moduli and modest limiting stretches.

We have shown that giant deformation of actuation is achievable for an elastomer with a stress-stretch curve of a desirable form: the elastomer is compliant at small stretches and then stiffens steeply at modest stretches. Such an elastomer either eliminates or survives the snap-through electromechanical instability, and reaches a stable state before electrical breakdown. It is hoped that this theory will help in the experimental search for dielectric elastomers capable of giant deformation of actuation.

This work is supported by NSF through a grant on Soft Active Materials (CMMI-0800161), by DARPA through a contract on Programmable Matter (W911NF-08- 1-0143), and by the Kavli Institute at Harvard University.

*suo@seas.harvard.edu

[1] P. Brochu and Q. B. Pei, Macromol. Rapid Commun. **31**, 10 (2010).
[2] F. Carpi, D. De Rossi, R. Kornbluh, R. Pelrine, and P. Sommer-Larsen, *Dielectric Elastomers as Electromechanical Transducers* (Elsevier, Oxford, 2008).
[3] G. Kovacs, L. During, S. Michel, and G. Terrasi, Sens. Actuators A, Phys. **155**, 299 (2009).
[4] I. A. Anderson, T. Hale, T. Gisby, T. Inamura, T. McKay, B. O'Brien, S. Walbran, and E. P. Calius, Appl. Phys. A **98**, 75 (2010).
[5] S. E. Park and T. R. Shrout, J. Appl. Phys. **82**, 1804 (1997).
[6] Q. M. Zhang, V. Bharti, and X. Zhao, Science **280**, 2101 (1998).
[7] M. Zhenyl, J. I. Scheinbeim, J. W. Lee, and B. A. Newman, J. Polym. Sci. B **32**, 2721 (1994).
[8] R. E. Pelrine, R. D. Kornbluh, and J. P. Joseph, Sens. Actuators A, Phys. **64**, 77 (1998).
[9] R. Pelrine, R. Kornbluh, Q. B. Pei, and J. Joseph, Science **287**, 836 (2000).
[10] S. M. Ha, W. Yuan, Q. B. Pei, R. Pelrine, and S. Stanford, Adv. Mater. **18**, 887 (2006).
[11] R. Shankar, T. K. Ghosh, and R. J. Spontak, Adv. Mater. **19**, 2218 (2007).
[12] C. Keplinger, M. Kaltenbrunner, N. Arnold, and S. Bauer, Proc. Natl. Acad. Sci. U.S.A. **107**, 4505 (2010).
[13] T. Blythe and D. Bloor, *Electrical Properties of Polymers* (Cambridge University Press, Cambridge, England, 2005).
[14] K. H. Stark and C. G. Garton, Nature (London) **176**, 1225 (1955).
[15] X. H. Zhao and Z. G. Suo, Appl. Phys. Lett. **91**, 061921 (2007).
[16] Y. C. Fung, *Biomechanics* (Springer, New York, 1993).
[17] K. Bertoldi and M. C. Boyce, J. Mater. Sci. **42**, 8943 (2007).
[18] Q. B. Pei (private communication).
[19] T. Hirai, J. Intell. Mater. Syst. Struct. **18**, 117 (2006).
[20] Z. G. Suo and J. Zhu, Appl. Phys. Lett. **95**, 232909 (2009).
[21] X. H. Zhao, W. Hong, and Z. G. Suo, Phys. Rev. B **76**, 134113 (2007).
[22] X. H. Zhao and Z. G. Suo, J. Appl. Phys. **104**, 123530 (2008).
[23] G. Kofod, P. Sommer-Larsen, R. Kronbluh, and R. Pelrine, J. Intell. Mater. Syst. Struct. **14**, 787 (2003).
[24] M. Wissler and E. Mazza, Sens. Actuators A, Phys. **138**, 384 (2007).
[25] J. S. Plante and S. Dubowsky, Int. J. Solids Struct. **43**, 7727 (2006).
[26] C. Keplinger, M. Kaltenbrunner, N. Arnold, and S. Bauer, Appl. Phys. Lett. **92**, 192903 (2008).
[27] M. Kollosche, M. Melzer, A. Becker, H. Stoyanov, D. N. M. Carthy, H. Ragusch, and G. Kofod, Proc. SPIE Int. Soc. Opt. Eng. **7287**, 728729 (2009).
[28] S. M. Ha, M. Wissler, R. Pelrine, S. Stanford, G. Kovacs, and Q. Pei, Proc. SPIE Int. Soc. Opt. Eng. **6524**, 652408 (2007).
[29] E. M. Arruda and M. C. Boyce, J. Mech. Phys. Solids **41**, 389 (1993).
[30] L. R. G. Treloar, *The Physics of Rubber Elasticity* (Clarendon Press, Oxford, 1975).